
*17th World Conference on Earthquake Engineering, 17WCEE*
*Sendai, Japan - September 13th to 18th 2020*

# A Practical Seismic Design Approach of Low-rise Tension-only Bracing Steel Frames with Self-Centering Panels

Junlin Li(1), Wei Wang(2)

(1) *PhD student, State Key Laboratory of Diaster Reduction in Civil Engineering, Tongji University, junlinli@tongji.edu.cn*
(2) *Professor, State Key Laboratory of Diaster Reduction in Civil Engineering, Tongji University, weiwang@tongji.edu.cn*

## *Abstract*

This paper develops a practical seismic design approach for an emerging lateral force resisting system consisting of self-centering panels and steel strip braces. The system combines the favorable re-centering feature of conventional self-centering building frames and the high stiffness and energy absorption capacity of concentrically braced frames. The system also overcomes the detrimental frame expansion effect that occurs in conventional self-centering building frames. Following the proposed design approach, multiple designs to achieve different performance objectives were performed for a representative three-story building in which the considered lateral force resisting system is used to resist the seismic forces. Nonlinear response history analyses were performed for the designs to evaluate the applicability and adequacy of the proposed design approach. Based on the analyses conducted in this research, it was found that the considered system designed using the proposed approach can meet both transient and residual inter-story drift requirements specified for a selected performance objective. While an initial design per the proposed design approach may be inadequate, the re-design strategy recommended can help transform the design to an acceptable after only one round of modification. Moreover, the proposed approach remains applicable for different performance objectives. Further, the high-mode effect appears nonnegligible in the considered system and this effect should be considered in the proposed approach through the use of the lateral distribution factor of seismic forces specifically for self-centering systems.

*Keywords: Self-centering; Energy absorbing; Design; Tension-only braces.*

 



## 1. Introduction

While past investigations have confirmed that conventional code-compliant steel building frames can exhibit the ductile behavior and achieve the intended performance objectives [1], some recent earthquakes revealed that these systems may experience the damage that is expensive, inconvenient, and even impossible to repair [2]. To achieve improved post-earthquake reparability in steel buildings, numerous types of steel building frames having the self-centering feature have been proposed and investigated [3]. Conceptually, introduction of the self-centering action into a multiple-story system helps eliminate its residual inter-story drifts after a severe earthquake, which helps create a satisfactory condition for the post-earthquake repair.

In this research, the authors focused on a new type of steel lateral force resisting system proposed to overcome the abovementioned limitations of the conventional self-centering steel building frames with post-tensioned beam-to-column connections. As will be described in detail in Section 2, the new system consists of self-centering panels and tension-only braces. The objective of this research was to develop and validate a practical yet adequate seismic design approach for the system to achieve performance objective.

The following first describes the system. Next, the design approach is presented. As part of the proposed design approach, the strategies for design iterations which become necessary when a trial design fails to meet the requirement associated with the selected performance objective are also presented. To validate the proposed design approach, a representative demonstration building is introduced, designed using the proposed design approach, and analyzed through nonlinear Response History Analyses (RHA). Based on the results from RHA, adequacy of the proposed design approach is addressed followed by the recommendations for implementing the design approach.

## 2. Description of the considered system

### 2.1 Major components

As depicted in Fig. 1, the considered steel lateral force resisting system consists of a multiple-bay boundary frame in which the self-centering panels and steel strip braces are installed. Simple beam-to-column connections consisting of the shear tabs with one interior bolt hole of standard size and two exterior bolt holes slotted along the longitudinal direction of the beam are adopted in the boundary frame. Note that the slotted bolt holes help eliminate the bearing failure in the high strength bolts or bolt holes caused by the expected connection rotations.

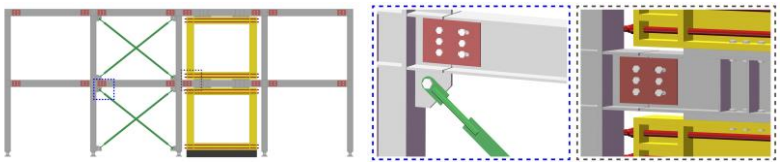

(a) Elevation of the considered system (b) Connections of the considered system

Fig. 1– Illustration of the considered system.

The self-centering panel is essentially a single-story single-bay frame with conventional post-tensioned beam-to-column connections. Each self-centering panel is installed to the boundary frame through high-strength bolts that connect the flanges of the panel beams and these of the frame beams or the foundation as Fig. 1a shows. When the system sways under earthquake loading, the frame expansion effect only occurs in the self-centering panels and will not spread into the boundary frame, eliminating the failures in the diaphragm/floor slab that were observed in the conventional self-centering building frames [4]. Beyond the self-centering panel, steel strip braces are installed to the considered system to dissipate hysteretic energy and provide additional lateral stiffness and strength. Each steel strip brace actually exhibits the tension-only behavior due to its extremely large slenderness ratio associated with the weak axis. Each strip brace is installed to the boundary frame through bolted connections as shown in Fig. 1b.



 



### 2.2 Demonstrated advantages and nonlinear behavior

Cyclic tests on the full-scale single-story specimens of the considered system were recently performed [5]. The experimental investigation confirmed that the considered system can exhibit the expected self-centering behavior without causing the frame expansion effect in the boundary frame [5, 6]. Moreover, the tests confirmed the tension-only behavior and post-earthquake replaceability of the strip braces [5]. The demonstrated advantages of the considered system [5] include the following. First, similar to the braces in conventional concentrically braced frames, the strip braces are efficient in increasing the system lateral stiffness and strength. Second, the strip braces buckle and subsequently exhibit negligible resistances during the unloading excursion for which they do not compromise the self-centering action of the system. Last but not least, recommendations for simulating the nonlinear behavior of the considered system in computer models are available in literature [7].

Taking a single-story example of the considered system (which is similar to the specimens tested in the past experimental study [5]) for consideration, Fig. 2 further illustrates the loading, unloading and reloading behavior of the self-centering panel under the cyclic loading excursions in one direction. As Fig. 2a shows, formation of the connection gap opening mechanism results in the stiffness degradation in the self-centering panel.

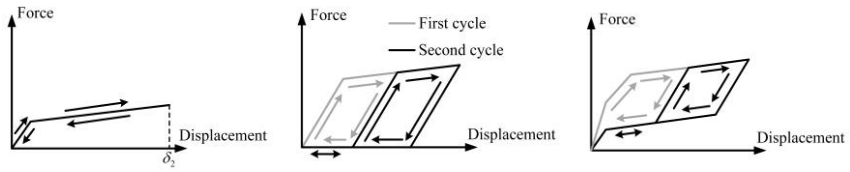


(a) The response of the self-centering panel (b) The response of the system due to the strip braces (c) The combined response of the system

Fig. 2– Illustration of the hysteretic response of the considered system

Fig. 2b sketches the loading, unloading, and reloading behavior of the steel strip braces under cyclic loading excursions in one direction. When the lateral displacement demand is large enough, the strip brace in compression buckles and develops a negligible contribution to the system lateral resistance while the other one in tension is permanently elongated. Accordingly, the steel strip braces do not contribute to the system lateral resistance unless the lateral displacement demand on the system exceeds the highest value ever experienced in that direction. Fig. 2b also reveals that the total energy dissipated by a strip brace is independent on the number of loading cycles it experiences. In fact, the total energy absorbed only depends on the largest elongation ever experienced by the brace.

Fig. 2c illustrates the behavior of the example single-story system which essentially combines the loading, unloading and reloading responses shown in Figs. 2a and 2b. As shown, combination of the self-centering panel and the strip braces enables the considered system to exhibit much higher lateral stiffness, lateral strength and energy dissipation while maintaining the favorable self-centering feature.

## 3. Development of a seismic design approach

To successfully achieve the intended seismic performance in the considered system, a practical yet adequate design approach is needed. This section presents the critical steps of a design approach developed for the considered system.

### 3.1 Design procedure

For an n-story example of the proposed system, the proposed design approach can be implemented through the following steps:



 



Step 1. Calculate the ductility demand on the strip braces associated with the allowable inter-story drift, $\mu_a$, as below:

$$\mu_a = \frac{\theta_a}{\theta_{by}} \tag{1}$$

$$\theta_{by} = \frac{2F_{by}}{E\sin(2\phi_b)} \tag{2}$$

where $\theta_a$ = allowable inter-story drift ratio specified in the applicable building code; $\theta_{by}$ = inter-story drift ratio associated with initial yielding of the strip braces; $F_{by}$ = yield strength of the steel of strip braces; $E$ = modulus of elasticity of steel; and $\phi_b$ = orientation angle of the strip braces relative to the horizontal direction.

Note that $\theta_{by}$ varies from story to story when story height in the considered example does not remain constant. In such a case, the minimum value of $\theta_{by}$ in the system should be used in Eq. (1).

Step 2. Assuming that the system develops the allowable inter-story drift ratio, $\theta_a$, and its inter-story drifts are uniformly distributed along the vertical direction, calculate the mass and displacement associated with its first vibration mode, $M_e$ and $\Delta_d$, respectively, as:

$$M_e = \frac{\sum_{i=1}^{n} m_i \Delta_i}{\Delta_d} \tag{3}$$

$$\Delta_d = \frac{\sum_{i=1}^{n} m_i \Delta_i^2}{\sum_{i=1}^{n} m_i \Delta_i} \tag{4}$$

where $m_i$ = seismic reactive mass of the $i^{th}$ story; and $\Delta_i$ = lateral displacement of the $i^{th}$ floor that can be calculated as:

$$\Delta_i = h_i \theta_a \tag{5}$$

in which: $h_i$ = elevation of the $i^{th}$ floor.

Step 3. Select the fundamental period of the system, T1, from the following relation:

$$\Delta_d = C_d(\mu = \mu_a,\ T_1) S_d(T_1) \tag{6}$$

where $S_d$ ($T_1$) = spectral response displacement at $T_1$ identified from the 5% damped linearly elastic design basis earthquake (DBE) spectrum; and $C_d$ ($\mu$, $T_1$) = displacement response adjustment factor which converts $S_d$ ($T_1$) into $\Delta_d$, i.e., the parameter converting the displacement response of a 5% damped linearly elastic single-degree-of-freedom (SDOF) system with the vibration period of $T_1$ into the first-mode displacement of the considered system.

Step 4. Determine the vertical distribution factor of seismic forces, $C_{v,i}$. As reported in past investigations, the high-mode effect in multiple-story self-centering systems are often remarkable. Based on the recommendations from Chao et al. [8] and others [9-11], the following equation which considers the high-mode effect in multiple-story self-centering systems is recommended for calculating $C_{v,i}$:

$$C_{v,i} = (p_i - p_{i+1}) \left( m_n h_n \Big/ \sum_{j=1}^{n} m_j h_j \right)^{0.75T_1^{-0.2}} \tag{7}$$



 



$$p_i = \left( \sum_{j=i}^{n} m_j h_j \Big/ m_n h_n \right)^{0.75 T_1^{-0.2}} \tag{8}$$

Step 5. Calculate the design base shear $V_u$ as:

$$V_u = V_b + V_{P\text{-}\Delta} \tag{9}$$

where $V_b$ = base shear associated with the first vibration mode of the system; and $V_{P\text{-}\Delta}$ = additional base shear due to the P-Δ effect in the system.

Similar to the conventional systems, $V_b$ can be estimated as:

$$V_b = M_e S_a(T_1) / R(\mu, T_1) \tag{10}$$

where $R(\mu, T_1)$ = response modification factor; and $S_a(T_1)$ = spectral response acceleration at $T_1$ identified from the 5% damped linearly elastic DBE design spectrum.

Note that $R(\mu, T_1)$ for the proposed system (which is an emerging system) is not reported in the existing literature. The authors developed an empirical model for $R(\mu, T_1)$ at the early stage of this research. More information about the model will be presented in Section 3.2. In addition, $V_{P\text{-}\Delta}$ depends on the inter-story drift responses and distribution of the seismic reactive masses in the considered system. Up to the allowable inter-story drift ratio (i.e. $\theta_a$), $V_{P\text{-}\Delta}$, can be computed as:

$$V_{P\text{-}\Delta} = \frac{\sum_{i=1}^{n} m_i g h_i \theta_a}{\sum_{i=1}^{n} C_{v,i} h_i} \tag{11}$$

where g = gravitational acceleration.

Step 6. Determine the seismic design lateral force at the $i^{th}$ floor, $F_i$, and the seismic design story shear at the $i^{th}$ story, $V_i$, respectively, as:

$$F_i = C_{v,i} V_u \tag{12}$$

$$V_i = \sum_{j=i}^{n} F_j \tag{13}$$

Step 7. Assigning 100% of the story shear to the strip braces at each story, i.e., assuming that $V_i$ is solely resisted by the tension-only braces at the $i^{th}$ story, size these braces. Note that the self-centering panels also contribute to the lateral resistance of the system. However, their beneficial contributions are conservatively neglected here for simplicity.

Step 8. Design the self-centering panel at each story. As described in Section 2, in spite of their strength and stiffness, the tension-only braces do not affect the self-centering feature of the system. Accordingly, designs of the self-centering panels and the tension-only braces are not coupled. However, it is assumed here that the ratio of the initial stiffness of a self-centering panel to that of the tension-only braces at the same story remains constant along the height of the system. Based on the input from the industry advisory members of this project, the ratio of one third appears practical for the low-rise systems.

Step 9. Based on the tension-only braces and self-centering panels designed in Step 8, design the boundary frame members according to the capacity design principle to ensure that the boundary frame remains fully elastic under the expected earthquake excitations.



 



Step 10. Perform the eigen-value analysis and verification RHA to obtain the actual fundamental period $T_1$ and the inter-story drift responses of the designed system, respectively. Amplify $V_u$ , update $C_{v,i}$ based on Eq. (7) and the actual fundamental period obtained from the eigen-value analysis, and repeat Steps 6 to 10 to re-design the system unless the results from the verification RHA suggest adequacy of the design (i.e., meet the transient inter-story drift requirement associated with the selected performance objective). Note that the strategies to amplify $V_u$ will be discussed in detail in Section 3.3.

## 3.2 Discussions on $R$ ($\mu$, $T_1$) and $C_d$ ($\mu$, $T_1$)

As described in Section 3.1, $R$ ($\mu$, $T_1$) and $C_d$ ($\mu$, $T_1$) are needed to initiate the design process. The empirical models for $R$ ($\mu$, $T_1$) and $C_d$ ($\mu$, $T_1$) were established based on the results from the RHA of the SDOF systems capturing the first-mode vibrations of the considered systems. Fig. 3 schematically shows the SDOF system. As shown, the SDOF system has two nonlinear springs (denoted as Springs A and B, respectively) and a dashpot in parallel which capture the strip braces, the self-centering panels, and the structural damping in the considered system, respectively.

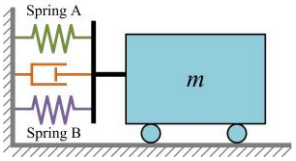


Fig. 3– Illustration of the single degree-of-freedom system

The following assumptions were made for the SDOF system. First, it was assumed that the initial stiffness of Spring B is one third of that of Spring A. In addition, the displacement associated with the gap opening action in Spring B was assumed to be one quarter of the yield displacement of the Spring B. Moreover, the mass proportional Raleigh damping of 5% was assumed for the SDOF system. Further, the period of the SDOF system was varied from 0.2 sec to 3.0 sec in increments of 0.1 sec. Last, the far-field ground motions considered in the ATC 63 project [12] were used for the analyses of the SDOF systems. It is important to note that the abovementioned assumptions are not always applicable to a given design case. These assumptions were made to demonstrate how the $R$ ($\mu$, $T_1$) and $C_d$ ($\mu$, $T_1$) models can be established to initiate the design process. If needed, the models for $R$ ($\mu$, $T_1$) and $C_d$ ($\mu$, $T_1$) can be similarly established for other analysis parameter ranges and/or combinations. Beyond the SDOF system shown in Fig.3, a 5% damped linearly elastic SDOF system with its period varied in the same manner was analyzed as a reference. By definition, $R$ ($\mu$, $T_1$) can be calculated as:

$$R(\mu,\ T_1) = \frac{F_e}{F_{yA}} \tag{14}$$

where $F_{yA}$ = strength of spring A which represents the strength contribution of the tension-only braces in the SDOF system shown in Fig. 3; and $F_e$ = seismic force demand on the reference linearly elastic SDOF system.

At a considered period, $T_1$, adjust $F_{yA}$ in the SDOF system shown in Fig. 3 until the ductility demand on the system, $\mu$, reaches a target value; then $R$ ($\mu$, $T_1$) can be calculated based on Eq. (14). Repeating this process for all the ground motions and all the considered periods gives a database of $R$ ($\mu$, $T_1$). Through regression analyses, an empirical model of $R$ ($\mu$, $T_1$) was established as:

$$R(\mu,\ T_1) = \left\{3\mu\left[1 - \frac{0.3}{\exp(T_1 - f)^2}\right]\right\}^{\exp\left(cT_1^{-d}\right)} \tag{15}$$

where

$$f = 0.0045\mu^2 - 0.1509\mu + 2.3944 \tag{16}$$



 



$$c = -0.0062\mu^2 + 0.1133\mu - 0.7431 \tag{17}$$

$$d = -0.0042\mu^2 + 0.0914\mu + 0.1302 \tag{18}$$

Fig. 4 compares predictions from Eq. (15) with the medians from the RHA. Moreover, as defined, $C_d$ ($\mu$, $T_1$) which converts the displacement response of the linearly elastic SDOF system into that of the corresponding nonlinear SDOF system which is shown in Fig. 3 and represents the considered system can be derived as:

$$C_d(\mu, T_1) = \frac{4\mu}{3R(\mu, T_1)} \tag{19}$$

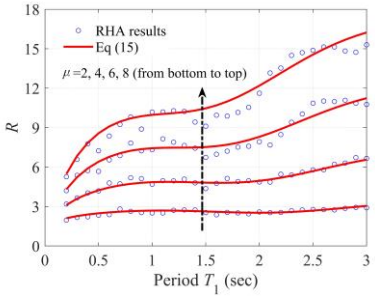


Fig. 4– The $R$-$\mu$–$T_1$ relationship: the RHA results vs. the regression model

The $R$ ($\mu$, $T_1$) and $C_d$ ($\mu$, $T_1$) models established above can be used in Step 2 of the design approach described in Section 3.1. Note that these models were established not to quantitively capture the nonlinear response properties of the considered system through the analysis results from the simple SDOF systems. In fact, it is challenging to simply use a SDOF system to perfectly capture the complicated responses of a multiple-story example of the considered system. However, these models help initiate the design in the right direction. When a trial design based on these models fails to achieve the expected performance objective, the iteration strategies for re-design presented in Section 3.3 should be used.

### 3.3 Strategies for design iterations

When the results from the verification RHA indicate that an initial design fails to meet the requirements associated with a selected design objective, it is necessary to amplify the design base shear and re-design the system.

Among the insufficient stories in the initial design, i.e., these in which the transient inter-story drift responses exceed the allowable inter-story drift, the least adequate story, denoted as the $m^{th}$ story, is identified from the following equation:

$$\frac{E_m}{\alpha_m} = \max\left(\frac{E_1}{\alpha_1}, \cdots \frac{E_i}{\alpha_i} \cdots, \frac{E_n}{\alpha_n}\right) \tag{20}$$

$$\alpha_i = \sum_{j=i}^{n} C_{v,j} \tag{21}$$

where $E_i$ = energy absorbed by the strip braces and self-centering panel in the $i^{th}$ story under its peak transient inter-story drift.

Strength of the least adequate story should be minimally increased to the level which ensures its energy absorption under the allowable inter-story drift specified in the applicable building code (i.e., when the strip braces in the story are under the ductility demand $\mu_a$) to be the same as the energy that absorbed in the originally designed story under its maximum transient inter-story drift (i.e., when the braces in the story are under $\mu_{max}$



 



where $\mu_{max}$ denotes the ductility demand on the strip braces in the least adequate story under the maximum transient inter-story drift). Fig. 5a compares the story shear versus brace ductility demand curves of the least adequate story before and after the story shear adjustment. As shown, the abovementioned story shear amplification is based on the equal energy criterion. It essentially requires the area below the curve of the re-design (which has a higher strength and a lower brace ductility demand, $V_{u2}$ and $\mu_a$) to be the same as that of the original design (which has a lower story strength but a higher brace ductility demand, $V_{u1}$ and $\mu_{max}$). Mathematically, the story shear amplification factor due to the equal energy criterion, $\beta_E$, can be derived as:

$$\beta_E = 1 + \frac{(\mu_{max} - \mu_a)\left[\alpha_b(\mu_{max} + \mu_a - 2) + 2\right]}{1 + 2(\mu_a - 1) + \alpha_b(\mu_a - 1)^2} \geq 1 \tag{22}$$

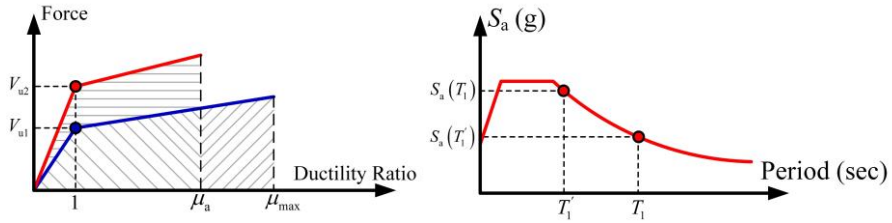


(a) The equal energy criterion (b) Increase in spectral demand due to the period shortening effect

Fig. 5– Illustrations of the strategies for design iterations

Notably, while $\beta_E$ is derived for the least adequate story, it should be actually used to amplify the shears in all stories, i.e., it should be used to amplify the base shear, since strengthening the least adequate story alone will concentrate the ductility demands in other less adequate stories. Conceptually, the base shear amplified by $\beta_E$ tends to lead to larger braces and a higher lateral stiffness in the system which accordingly shortens its fundamental period. The fundamental period, $T_1$, considered in the original design and the shortened fundamental period due to the application of $\beta_E$, denoted as $T_1'$, satisfy the following equation:

$$T_1' = \frac{T_1}{\sqrt{\beta_E}} \tag{23}$$

As Fig. 5b shows, depending on the shape of the design spectrum, the shortened fundamental period can also cause an amplification in the spectral response acceleration demand which consequently amplifies the design base shear by the following factor, $\beta_T$:

$$\beta_T = \frac{S_a(T_1')}{S_a(T_1)} \geq 1 \tag{24}$$

Combining $\beta_E$ and $\beta_T$, the factor for amplifying the base shear for re-design, $\beta$, is determined as:

$$\beta = \beta_T \beta_E \tag{25}$$

## 4. Validation of the seismic design approach

A demonstration building was considered to assess the adequacy of the design approach presented in Section 3. Multiple designs for the demonstration building were obtained using the proposed approach to achieve a performance objective. Computer models of these designs were developed and nonlinear RHA were performed to confirm if the anticipated performance objective can be successfully achieved. The following presents the basic information of the demonstration building, the selected performance objective, detailed designs based on the proposed approach, and RHA results of these designs.



 



## 4.1 Demonstration building

A three-story building frame in Pomona, California (which was considered in a previous investigation for other research purposes [13]) was revisited as the demonstration building in this research. The building has a constant story height of 3810 mm. The design spectral response acceleration parameter in the short period range and that at a period of 1.0 sec, i.e., $S_{DS}$ and $S_{D1}$, are 1.0g and 0.6g, respectively. The DBE design spectrum is shown in Fig. 6a.

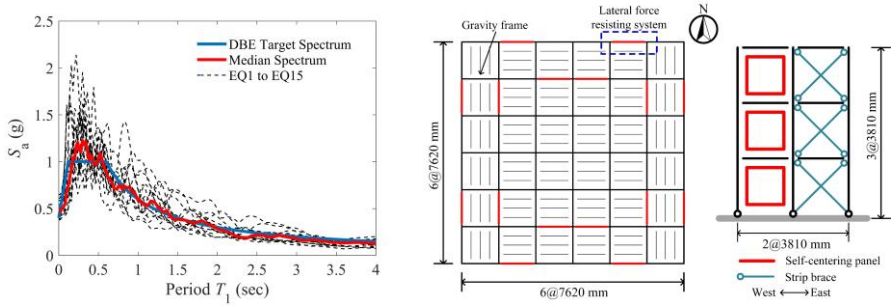


(a) Comparison of the spectra (b) Illustration of the demonstration building

Fig. 6– Information of the demonstration building

Fig. 6b shows the floor plan of the demonstration building. As shown, eight identical lateral force resisting systems are symmetrically arranged along each horizontal direction. Note that original design of the building also includes a basement. For simplicity, the basement was neglected and all columns were assumed to be pinned to the ground in this research. Fig. 6b also shows the elevation of a selected lateral force resisting system in which the considered system is implemented. The tributary seismic reactive weights of the third story is 1021.3 kN while these of the other stories are 1404.8 kN.

Q345 steel and Q420 steel (which have the nominal yield strengths of 345 MPa and 420 MPa, respectively) were assumed for the boundary frame members and the strip braces, respectively. Note that a strain hardening ratio of 2% was assumed for the Q420 steel. Moreover, it was assumed that the beams and columns in the self-centering panels are made of Q 345 steel. The yield strength of the tendons in the self-centering panels was assumed to be 1860 MPa. For simplicity and owing to symmetry, only one lateral force resisting system shown in Fig. 6b was designed and analyzed for the demonstration building. To evaluate the applicability of the proposed design approach, one performance objective, denoted Objectives I was considered for the demonstrate building. Specifically, Objective I allows the maximum transient inter-story drift ratios of 0.012 rad in the demonstration building under the DBE excitations, respectively. Additionally, the two objectives require the residual inter-story drifts to be negligible (i.e., less than 0.002 rad) under the DBE excitations.

For comparison purpose, two designs were performed for selected performance objective, including one following the procedure described in Section 3.1 and the other based on the same procedure except that $C_{v,i}$ defined in the following equation and recommended in ASCE/SEI 7-16 [14] was used as an alternative to that defined in Eq. (7).

$$C_{v,i} = \frac{m_i h_i^k}{\sum_{j=1}^{n} m_j h_j^k} \tag{26}$$

where $k$ = an exponent related to the period as follows: $k$ = 1 for structures having a period of 0.5 sec or less; $k$ = 2 for structures having a period of 2.5 sec or more; and k shall be interpolated between 1.0 and 2.0 for structures having a period between 0.5 sec and 2.5 sec.

Note that Eq. (26) is recommended in ASCE/SEI 7-16 [14] for conventional lateral force resisting systems and it does not explicitly account for the influence of the high-mode effect on the vertical distribution



 



of seismic forces and the unique properties of self-centering systems. Comparison of the designs adopting Eqs. (7) and (26) helps address if the high-mode effect can be neglected in seismic design of the considered self-centering system.

### 4.2 Computer modeling and seismic excitations

The system shown in Fig. 6b was numerically modelled in *OpenSees* [15] based on the modelling recommendations from prior investigations [7]. Fig. 7 schematically shows the computer model.

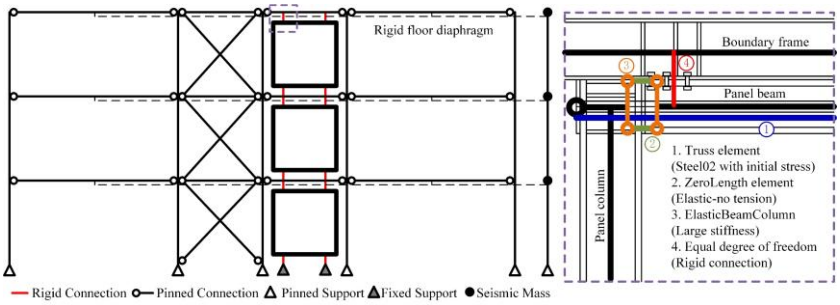


Fig. 7– Illustration of the computer model

The computer model of each design was analyzed using a set of 15 design-spectrum-matching far-field earthquake records selected from the online ground motion database of the Pacific Earthquake Engineering Research Center-Next Generation Attenuation (PEER-NGA) project (website: https://ngawest2.berkeley.edu/). As shown in Fig. 6a, the median linearly elastic response spectrum of the selected ground motions is practically compatible with the DBE design spectrum over the considered period range. Note that a 10-sec damped free vibration history was included at the end of each analysis to determine the residual inter-story drifts in the system.

### 4.3 Discussions of analysis results

Following the proposed design procedure, the initial periods selected based on Eq. (6) for Performance Objective I is 0.59 sec. Table 1 lists the critical details of the initial design of each considered case including the cross-section areas of the strip braces and the cross-section areas and initial stresses in the tendons. Fig. 8a shows the median peak transient inter-story drift ratios along the height of each initial design which were obtained from the nonlinear RHA. As shown, all the initial designs develop the median transient inter-story drift ratios higher than the limit required by the anticipated performance objective. As such, the initial designs were modified based on the strategies presented in Section 3.3.

Table 1- Summary of the initial designs and re-designs*

| Performance objective | Equation for $C_{v,i}$ | Story | Strip braces | Tendons in self-centering panels | |
|---|---|---|---|---|---|
| | | | Cross-section areas ($mm^2$) | Cross-section areas ($mm^2$) | Initial stresses (MPa) |
| I | Eq. (26) | 3 | 1398 (2731) | 489 (900) | 415 (415) |
| | | 2 | 2656 (5234) | 531 (970) | 540 (540) |
| | | 1 | 3265 (6486) | 627 (1185) | 560 (560) |
| | Eq. (7) | 3 | 1587 (2678) | 552 (883) | 415 (415) |
| | | 2 | 2728 (4743) | 546 (892) | 540 (540) |
| | | 1 | 3260 (5725) | 627 (1057) | 560 (560) |



 



* Information of the re-design is included the parentheses.

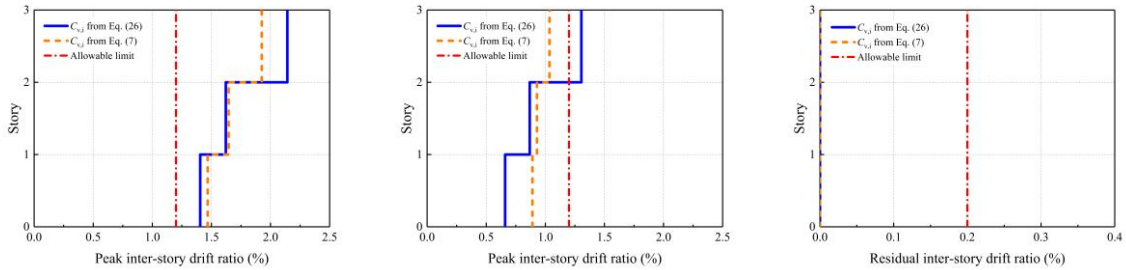


(a) Median transient inter-story drift ratios of the initial designs (b) Median transient inter-story drift ratios of the re-designs (c) Median residual inter-story drift ratios of the re-designs

Fig. 8– Median response of initial designs and re-designs

Table 1 also lists the re-designs of the considered cases after one round of update. Fig. 8b compares the median peak transient inter-story drift ratios of the re-designs. As shown, all the re-designs meet the requirements on transient inter-story drift ratios except for the one designed with $C_{v,i}$ determined from Eq. (26) to achieve Performance Objective I. Fig. 8c further presents the median residual inter-story drift ratios of the re-designs. As shown, all the re-designs developed negligible residual deformations as expected, demonstrating the favorable self-centering feature of the considered system.

## 5. Concluding remarks

This paper develops a seismic design procedure for an emerging lateral force resisting system consisting of self-centering panels and strip braces. Following the proposed design approach, multiple designs were performed for a representative three-story building to achieve anticipated performance objective. Among the designs, different equations for the vertical distribution factor of seismic forces recommended by past investigations and the applicable building code were considered. Nonlinear RHA were performed for the initial designs and re-designs to evaluate the applicability and adequacy of the proposed design approach. Based on the analyses conducted in this research, the following major conclusions may be drawn:

- Computer models developed in this research numerically confirms that the considered system preferably combines the re-centering feature of the conventional self-centering building frames and the energy absorption capacity and high initial stiffness of concentrically braced frames. If properly designed, the considered system can meet both transient and residual inter-story drift requirements.
- The proposed seismic design approach is adequate for the considered system. The design approach remains applicable for achieving expected performance objective.
- It was found that the initial designs obtained from the proposed approach may be inadequate. While design iterations may be needed, based on the re-design strategies recommended in the proposed design approach, the inadequate initial designs can converge to the acceptable ones after only one round of modification, suggesting the efficiency and effectiveness of the proposed design approach.
- The high-mode effect appears nonnegligible in the considered system. The vertical distribution factor of seismic forces recommended for conventional self-centering systems and considering the high-mode effect should be used in the proposed seismic design approach. Adoption of the vertical distribution factor of seismic forces for conventional lateral force resisting systems in the proposed design approach can cause less uniform and even unacceptable transient inter-story drift responses in the considered system and it should not be used in design of the considered system.



 



## 6. Acknowledgement

The financial supports from the Natural Science Foundation of China (NSFC) with Grant Nos. 51778459 and 51820105013 are gratefully acknowledged.

## 7. References

[1] Bruneau M, Uang CM, Sabelli R. Ductile Design of Steel Structures: McGrawHill; 2011.

[2] Cole G, Dhakal R, Turner F. Building pounding damage observed in the 2011 Christchurch earthquake. Earthquake Engineering & Structural Dynamics. 2012;41:893-913.

[3] Chancellor NB, Eatherton MR, Roke DA, Akbaş T. Self-Centering Seismic Lateral Force Resisting Systems: High Performance Structures for the City of Tomorrow. Buildings. 2014;4:520-548.

[4] MacRae G, Gunasekaran U. A concept for consideration of slab effects on building seismic performance. Proceedings of the New Zealand Society for Earthquake Engineering conference. New Zealand,2006.

[5] Wang W, Du X, Zhang Y, Chen Y. Experimental Investigation of Beam-Through Steel Frames with Self-Centering Modular Panels. Journal of Structural Engineering. 2017;143.

[6] Wang W, Kong J, Zhang Y, Chu G, Chen Y. Seismic Behavior of Self-Centering Modular Panel with Slit Steel Plate Shear Walls: Experimental Testing. Journal of Structural Engineering. 2018;144.

[7] Du X, Wang W, Chan TM. Seismic design of beam-through steel frames with self-centering modular panels. Journal of Constructional Steel Research. 2018;141:179-188.

[8] Chao SH, Goel SC, Lee SS. A seismic design lateral force distribution based on inelastic state of structures. Earthquake Spectra. 2007;23:547-569.

[9] Qiu CX, Zhu S. High-mode effects on seismic performance of multi-story self-centering braced steel frames. Journal of Constructional Steel Research. 2016;119.

[10] Qiu CX, Zhu S. Performance-based seismic design of self-centering steel frames with SMA-based braces. Engineering Structures. 2017;130:67-82.

[11] Clayton P, Berman J, Lowes L. Seismic Design and Performance of Self-Centering Steel Plate Shear Walls. Journal of Structural Engineering. 2012;138:22-30.

[12] FEMA. FEMA P695. Quantification of Building Seismic Performance Factors. Washington, DC: Federal Emergency Management Agency; 2009.

[13] Dong B. Large-scale Experimental, Numerical, and Design Studies of Steel MRF Structures with Nonlinear Viscous Dampers under Seismic Loading. Bethlehem, Pennsylvania: Lehigh University; 2016.

[14] ASCE. Minimum design loads for buildings and other structures: ASCE/SEI 7-16. American Society of Civil Engineers; 2017.

[15] Mazzoni S, McKenna F, Scott MH, Fenves GL. OpenSees Command Language Manual. Pacific Earthquake Engineering Research(PEER) Center; 2006.



 